Minimize leakage currents in Solar-PV systems with passive filters and fuzzy based voltage source converter

KATRAVATH SARITHA[1] |G RAMA KRISHNA[2]B.SHIVAJI

[1]Pg Scholar, Dept of EPS, Kodada Institute of Technology & Science for Women-Kodad, Telangana.

[2] Assistant Professor, Dept of EEE, Kodada Institute of Technology & Science for Women-Kodad,Telangana.

[3]Assoc Professor& HOD,Dept of EEE, Kodada Institute of Technology & Science for Women-Kodad,Telangana.

ABSTRACT: Due to grounding issues and fault operation of power converters parasitic capacitance are emerged in the closed path of grid connected PV systems. This undesired capacitance develops the leakage current within the PV modules and leads to degrade overall performance of the system. However, the quantity of this leakage current is low if it exists over time span place a significant loss. Particularly, for the commission of large scale PV system these leakage currents create the many power quality issues. To address this problem, design of passive filters is presented in this work. Additionally, for harmonic compensation, voltage source converter (VSC) operated with a fuzzy logic controller (FLC). The fuzzy membership decisions rules well operate the VSC and perform the harmonic compensation. The simulation results are exhibits that the proposed passive filters and fuzzy based VSC can reduce the impact of the leakage current in the PV systems. The proposed approach can be more efficient and improves the overall performance of Solar-PV system.

KEYWORDS: VSC, FLC, LEAKAGE CURRENTS, SOLAR, PASSIVE FILTER.

I.INTRODUCTION: Due to low maintenance, absent of gas emission and atmospheric features the adoption of solar energy conversion system (SECS) have been growing rapidly recently. A few advanced technologies stated [1] that is significantly reducing the initial costs of SECS. In this aspect, SECS-PV system installation is greater over the other alternative renewable energy (RE) sources.

The power produced from the SECS is highly intermittence and nonlinear nature.

To enhance the reliability of the SECS system it can be incorporated with the grid. However, these grid-interfaced SECS suffering with several issues [2] such as fault ride-through capability, leakage currents due to parasitic capacitances, magnetic interference, harmonics production due to adoption of various power converters, and grid synchronization problems.

Faulty ground or insulation, the space among PV module to ground and false switching operation of PV converters are prime source to develop the parasitic capacitance in the SECS. This parasitic capacitance are create unwanted path for flow the current in the SECS network. This leakage current exists over the time period it can degrades the performance of closed-loop SECS system. To overcome this problem, a transformer based converter circuit for SEC systems [3] is introduced. This can facilitates the galvanic isolation so that the influence of the leakage current is eliminated from the closed path. Despite the circuit becomes complex to control and cost effective.

Single-phase topologies such as H5 and H6 [3]-[4] have been suggested to mitigate leakage currents for grid integrated PV systems. However, these converter topologies simple to control, it requires additional semiconductor components. As results, increases losses and arises power quality issues. To address these short comings, optimized topologies such as H5, H-bridge zero-voltage state rectifiers [4], [5] and modified H8, and H9 [7]-[8] topologies have been established. With the modifying traditional full-bridge converter the impact of leakage current is reduce. However, these three-phase circuits includes with more no. of power semiconductor devices, gate drivers, and corresponding control scheme. It is very difficult to design control algorithm for modified full bridge circuits. Besides, the lack of these circuit topologies is no harmonic compensation capability when connected to the nonlinear loads**.**

Recently, many filtering techniques have been documented in the literature to mitigate the existence of leakage currents in electronic circuits. These filters typically provide a high impedance path to eliminate the impact of high-frequency components. In this direction, a filter-based solution is proposed in [9] to reduce the leakage currents. Similarly, modified LCL filters [10] have been suggested to attenuate leakage currents in grid-connected SECS-PV systems.

Mitigating leakage current is possible effectively with passive filters. These filters

structure contains with inductors and capacitors. While equipping passive filters within the SECS, typically near at the PCC. These filters reduce the high-frequency components of leakage currents. In addition in this paper, fuzzy-based VSCs are proposed. FLC control scheme handles nonlinear and uncertain systems well and widely suitable for grid integrated SECS. FLC mechanisms dynamically adjust the VSC's switching patterns and ensure optimal energy extraction from the PV modules. Subsequently, reduce leakage currents and enhance power quality.

II.PROPOSED SYSTEM: The passive clear out-primarily based solar PV array device required by using numerous grid codes is presented in this thesis to lessen leakage current. The manner of designing a clear out in detail is included, and frequency area analysis is used to locate the fine filter out parameters. In addition, the adaptive controller is integrated herein for the clean extraction of the fundamental components. In comparison to conventional algorithms, the adaptive controller has some of benefits, including a better price of convergence, excessive stability, and occasional complexity. The advantage of the supplied sun strength conversion gadget is as follows.

- € To reduce leakage present day in a grid-tied sun PV array machine without the use of additional semiconductor devices, the passive filter layout is proposed here. The filter out parameters are derived via discussing the in-depth, step-through-step design process. The effect of varying the clear out's parameters is also tested through the usage of the frequency domain evaluation. To acquire the goal of lowering leakage modern, the first-rate parameters are chosen.
- € The adaptive controller is integrated herein to extract the fundamental aspect of the burden present day which will provide harmonic reimbursement. The controller's stability analysis is likewise looked at to see how properly it works with sun power conversion systems.
- € In evaluation to trendy structures, the grid currents' total harmonic distortions (THDs) are within acceptable limits, making an allowance for balanced grid currents inspite of unbalanced nonlinear masses and adhering to IEEE std. 519 and IEEE std. 61727. The presented machine concurrently follows the mandate revised IEEE std. 519, IEC std. 61727, DIN std. Even beneath coupled nonlinear load, VDE-00126-1-1 and NB/T std. 320004 continue to be powerful.

- € The presented gadget's efficiency is confirmed by way of real-time hardware-in-loop performance. It plays satisfactorily in a variety of situations, consisting of abnormal grid situations, distribution static compensator (DSTATCOM) mode, load unbalancing, and variant in sun insolation..

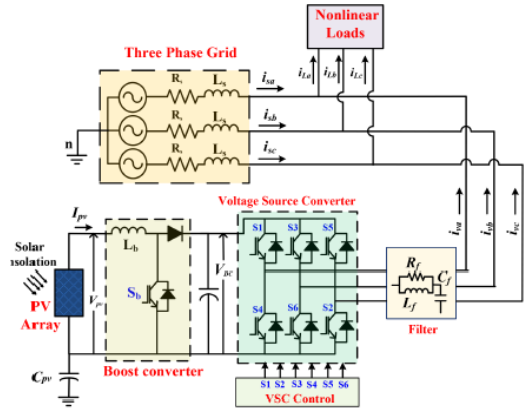

Fig. 1. Schematics of three-phase grid-tied solar energy conversion system.

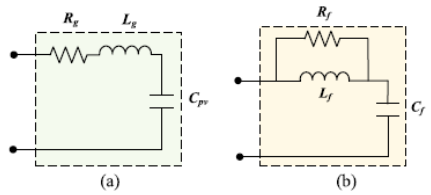

Fig. 2. Equivalent circuit of typical grid-tied solar energy conversion system and (b) Schematic of the presented filter.

The typical schematics of a sun strength conversion system are depicted in Fig. 1. Fig. 2(a) suggests the equivalent circuit of an average grid-interfaced sun PV device [26]. In Fig. 3(a), the equal circuit of the leakage current direction of a grid-tied sun PV array system's frequency area analysis is plotted. It can be located that the significance of the impedance supplied by the machine is substantially low for resonance frequency as depicted in Fig. 3(a). As a end result, it presents a direction with a decrease impedance and lets in the circuit's leakage current. Therefore, the passive filter out must be designed in this sort of way that it increases the impedance on the resonance frequency and enhances the gadget overall performance as depicted in Fig. 3. Fig. 2(b) shows the schematic diagram of the supplied passive filter out. The passive filter is coupled with the voltage supply converter to be able to suppress the switching voltage harmonics and cutting-edge harmonics. In addition, it reduces leakage cutting-edge with the aid of offering a course with higher impedance at the resonance frequency. The presented filter out consists of the parallel and collection mixture of resistor (Rf), inductor (Lf), and capacitor (Cf), which may be expressed using the second one-order switch feature. The filter's enter impedance (Zin) is expressed as,

$$Z_{in} = \frac{sR_fL_f}{R_f + sL_f} + \frac{1}{sC_f} \quad (1)$$

Eq. (1) can be expressed by rearranging the several terms as,

$$Z_{in} = \frac{\frac{s^2}{1/L_fC_f} + \frac{s}{R_f/L_f} + 1}{(sC_f)\left(1 + \frac{s}{R_f/L_f}\right)} \quad (2)$$

From (2), the detailed location of poles and zeros are described in Table II. Whereas, $\omega_1 = R_f/L_f$ and $\omega_2 = 1/\sqrt{L_fC_f}$. The damping ratio ($\delta$) can be expressed as,

$$2\delta\,\omega_2 = \frac{1}{R_fC_f} \Rightarrow \delta = \frac{\omega_2}{2\omega_1} = \frac{1}{2R_f}\sqrt{\frac{L_f}{C_f}} \quad (3)$$

The damping ratio performs an critical role throughout the transition on the nook

frequency. To suppress the resonance frequency, nook frequency (ω2) of zero need to be much less than the resonance frequency of the grid (fgrid). If the damping ratio is chosen zero.Five then impedance offered at corner frequency among low-frequency asymptote and high-frequency asymptote is premiere. During the transition from low-frequency asymptote to excessive-frequency asymptote, the low impedance notch can be seen at nook frequency if the damping ratio is less than 0.1. When the damping ratio is extra than 0.Five, the corner frequency transition impedance is better than in different cases. However, a essential thing is the impedance at the high-frequency asymptote, which may be comprehended thru three wonderful scenarios. It can be defined as follows. 1) Case-I: Let's recollect, damping ratio (δ) = zero.Five and calculated the clear out parameters are 251.32 Ω, 8 mH, and 126.65 nF, respectively. Fig. 3(a) suggests the bode plot for this designed filter. One can analyze that the designed filter presents extensively low impedance at high-frequency asymptote. As a end result, it makes it feasible to inject additives with higher frequencies into the grid-side community. Fig. 3(b) shows the frequency area analysis with the combination of clear out with sun power conversion system.

The presented impedance at higher frequency asymptote is quite low and it is able to bog down the system overall performance. 2) Case II: Assuming a damping ratio of one.Five, the filter resistance, inductance, and capacitance are calculated as 83.77, eight mH, and 126.Sixty five nF, respectively, the usage of (2) and (3). The frequency-domain bode plot for this designed clear out and the general system is illustrated in Fig. 3(a) and (b), respectively. Nonetheless, the development of impedance presented at excessive frequency asymptote is rather low in comparison to case-I. As a result, while compared to case-I, the standard leakage current value is drastically higher. 3) Case-III: Let's take into account, damping ratio (δ) = 0.1 and designed filter out resistance, filter inductance, and filter out capacitance are 1.25 kΩ, 8 mH, and 126.65 nF. The frequency-area plot for this designed clear out is plotted in Fig. 3(a). It suggests an outstanding response because it correctly eliminates the resonance factor from the grid and offers higher impedance for resonance frequency. In addition, the frequency area plot with the integration of this designed filter with an general system is verified in Fig. 3(b). One can study that it

gives a higher impedance trajectory at high-frequency asymptote compared to case-I and case-II. Hence, these filter out parameters are selected for the nice performance of the grid-tied sun PV array structures.

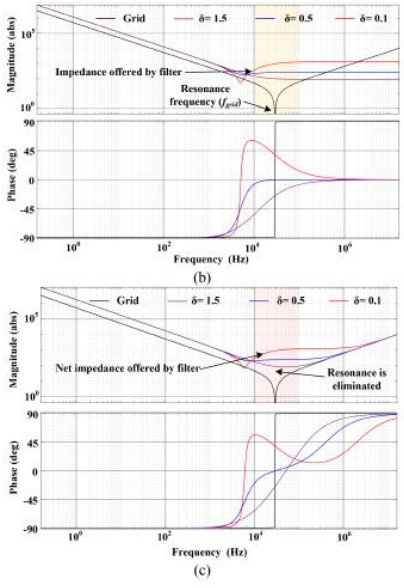

Fig. 3. Frequency domain analysis of (a) only filter (b) filter coupled solar energy conversion system.

Fig.4 shows the layout of grid connected SECS with passive filter. The solar and grid together fed power to the nonlinear loads. The circuit mainly composed with boost converter, VSC and passive filters. The optimal performance of the complete network depends on the operation of these power converters.

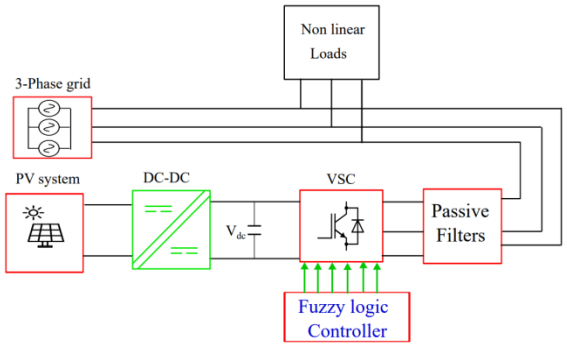

Fig.4 layout of grid integrated SECS with passive filter

III.SIMULATION RESULTS:

PROPOSED FLC RESULTS:

The MATLAB circuit of proposed grid connected SECS is depicted in fig.5. To validate the proposed control approach, a simulation study carried out for various operating conditions.

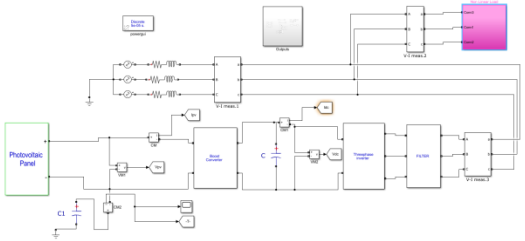

Fig.5 MATLAB circuit diagram of proposed SECS

Case 1: Performance of SECS under nominal condition

Fig 6(a) and fig 6(b) and illustrate the obtained simulation responses of grid voltages, grid currents When SECS with nonlinear loads under steady state condition. From the grid currents output waveform it is noticed that a transient oscillatory response during the initial phase, attributed to the stabilization of the DC bus voltage. Despite the presence of nonlinear loads, the grid

currents maintain a sinusoidal and balanced profile. Conversely, the load currents exhibit a characteristic nonlinear behavior, as depicted in the figure (see fig 6(c)).

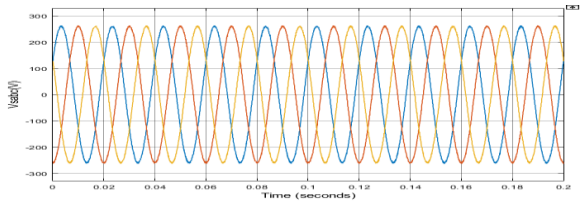

Fig.6a Grid voltage

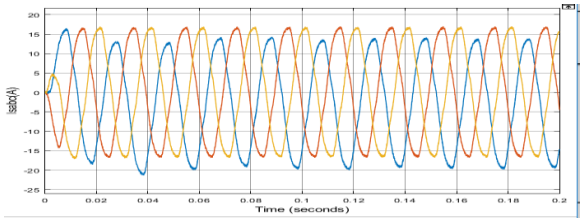

Fig.6b Grid current

From fig. 6(e) it is reveals that the DC bus voltage closely tracks the reference value, ensuring stable system operation. Furthermore, the system effectively extracts maximum power from the solar PV array, as evident from the dynamic behavior of the solar PV power in Figure 6(f).

Case 2: Performance of SECS under unbalanced load condition

Figures 7(a) and 8(b) present the system's response to an imbalanced load scenario.

When an imbalance occurs in the load network (suddenly removed load at one phase), the overall power consumption decreases. The resulting power imbalance is then accommodated by the grid-side network. This dynamic behavior is reflected in the grid current waveforms. The simulation responses of grid voltages, grid currents and load current are represented in fig.7a, fig.7b and fig.7c respectively.

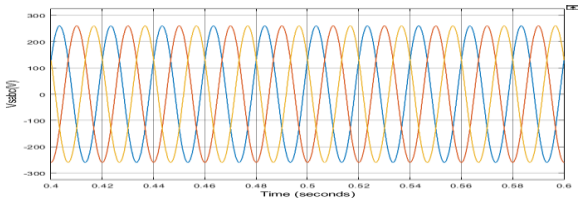

Fig.7a grid voltage

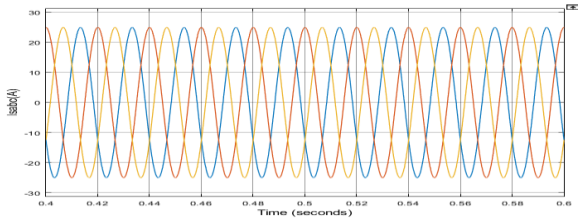

Fig.7b Grid current

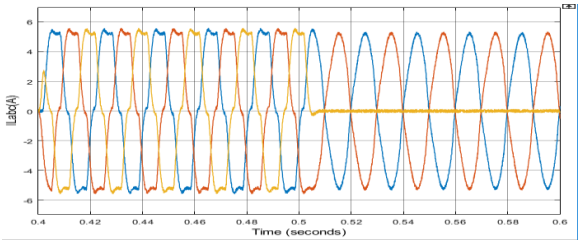

Fig.7c Load current

The VSC-coupled solar PV array system actively provides compensating currents (iv_{abc}) to maintain unity power factor at the grid interface. Even though power generated by Solar is not affected and DC link voltage also maintained at constant value.

This is further evidenced by the in-phase relationship between the grid voltage (vsa) and current (i_{sa}) in the 'a' phase. The simulation responses of VSC compensating currents, DC link voltage, and solar power and leakage currents are shown in fig.7d to

fig.7f respectively. The RMS value of leakage current is also restricted within the permissible limits.

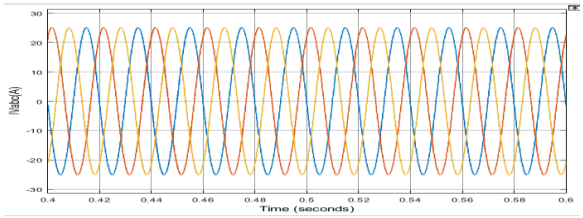

Fig.7d compensating current

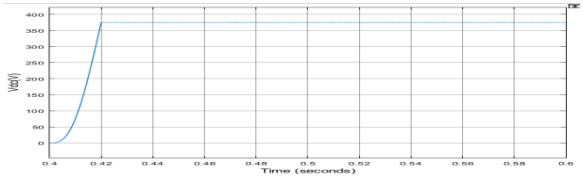

Fig.7e DC link voltage

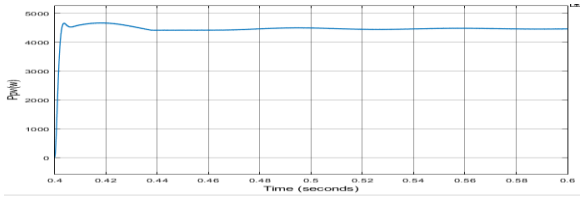

Fig.7e Solar power

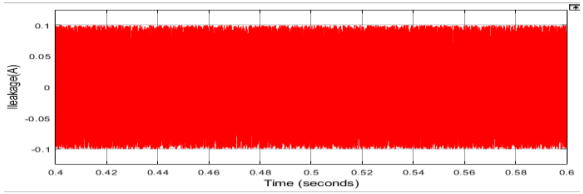

Fig.7f Leakage current

Case 3: Performance of SECS during varying solar insolation

In this case behavior of SECS at variable solar insolation is verified. A significant drop in solar power generation occurs at 0.5 seconds, due to decrease of solar irradiation from 1000 W/m² to 600 W/m².

As decrease in solar power generation results the magnitude of grid currents (see fig.8b) is also reduced. Although, the load power consumption remains unaffected during this event. The system consistently maintains unity power factor operation throughout the entire process, as evidenced by the in-phase relationship between grid voltage and current. The simulation responses of grid voltage and load current are shown in fig.8a and fig.8c

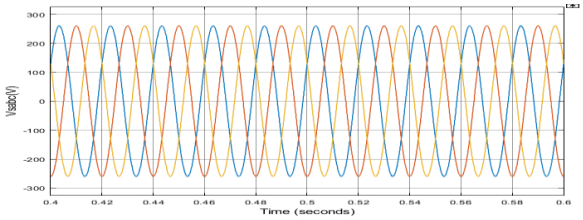

Fig.8a grid voltage

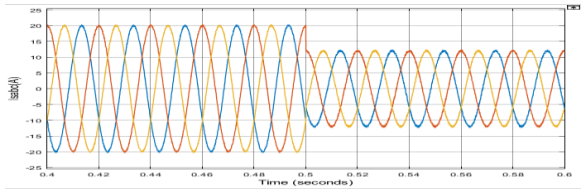

Fig.8a grid current

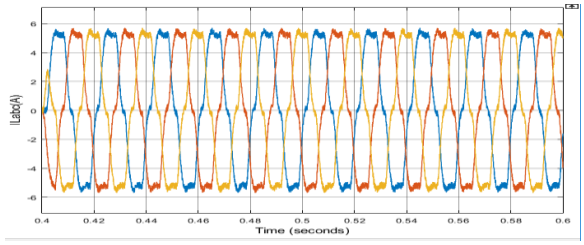

Fig.8c Load current

The DC bus voltage is effectively maintained at a constant level despite the reduction in solar irradiation. A significant drop in solar power generation occurs at 0.5 seconds, coinciding with the decrease in solar insolation. The obtained simulation responses of DC link voltage, PV power and

leakage current are depicts in fig.8d, fig.8e and fig.8f respectively. The RMS value of leakage current obtained within the acceptable limit.

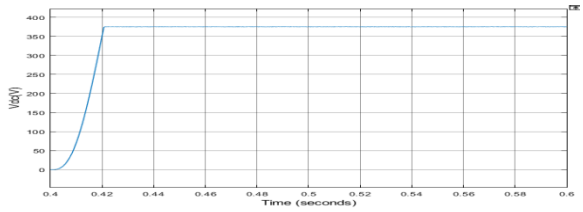

Fig.8d DC link voltage

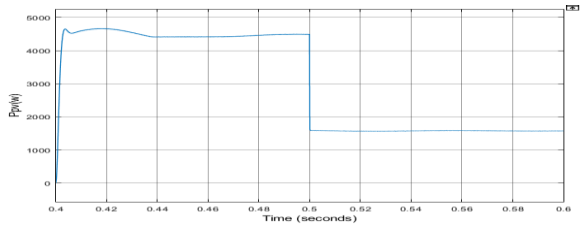

Fig.8e solar power

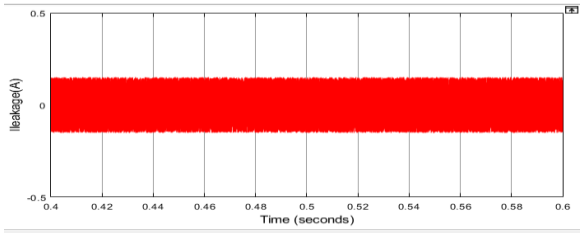

Fig.8f leakage current

IV.CONCLUSION:

The grid connected SECS is suffering from the parasitic capacitances. These capacitances cause to generate unwanted current paths results develop the leakage current. The existence leakage currents longer time span leads to power quality problems. To overcome this problem, a combination of passive filters and fuzzy-based VSCs is presented in this paper. Where the passive filters suppress the leakage currents in the network and FLC based VSCs responsible the current harmonic compensation. This novel approach offers a promising solution for mitigating leakage currents in grid connected SECS. From the simulation results it is proven that the proposed approach limits the leakage current as acceptable value and regulates the DC link voltage at steady state.

V.REFERENCES: [1] A. Molina-Garcia, J. Guerrero-Pérez, M. C. Bueso, M. Kessler, and E. Gómez-Lázaro, “A new solar module modeling for PV applications based on a symmetrized and shifted gompertz model,” IEEE Trans. Energy Convers., vol. 30, no. 1, pp. 51–59, Mar. 2015.

[2] R. Panigrahi, S. K. Mishra, S. C. Srivastava, A. K. Srivastava, and N. N. Schulz, “Grid integration of small-scale photovoltaic systems in secondary distribution network—A review,” IEEE Trans. Ind. Appl., vol. 56, no. 3, pp. 3178–3195, May/Jun. 2020.

[3] Power generation systems connected to the low-voltage distribution network—Technical minimum requirements for the connection to and parallel operation with low-voltage distribution networks, VDE-ARN 4105-2011, 2011.

[4] S. Mishra et al., "Enabling cyber-physical demand response in smart grids via conjoint communication and controller design," IET Cyber-Phys. System: Theory Appl., vol. 4, no. 4, pp. 291–303, Dec. 2019.

[5] N. G. Dhere, N. S. Shiradkar, and E. Schneller, "Evolution of leakage current paths in MC-Si PV modules from leading manufacturers undergoing high-voltage bias testing," IEEE J. Photovolt., vol. 4, no. 2, pp. 654–658, Mar. 2014.

[6] M. Rabiul Islam, A. M. Mahfuz-Ur-Rahman, K. M. Muttaqi, and D. Sutanto, "State-of-the-art of the medium-voltage power converter technologies for grid integration of solar photovoltaic power plants," IEEE Trans. Energy Convers., vol. 34, no. 1, pp. 372–384, Mar. 2019.

[7] A. Ahmed, M. S. Manoharan, and J. Park, "An efficient single-sourced asymmetrical cascaded multilevel inverter with reduced leakage current suitable for single-stage PV systems," IEEE Trans. Energy Convers., vol. 34, no. 1, pp. 211–220, Mar. 2019.

[8] K. S. Kumar, A. Kirubakaran, and N. Subrahmanyam, "Bidirectional clamping-based H5, HERIC, and H6 transformerless inverter topologies with reactive power capability," IEEE Trans. Ind. Appl., vol. 56, no. 5, pp. 5119–5128, Sep./Oct. 2020.

[9] M. N. H. Khan, M. Forouzesh, Y. P. Siwakoti, L. Li, T. Kerekes, and F. Blaabjerg, "Transformerless inverter topologies for single-phase photovoltaic systems: A comparative review," IEEE Trans. Emerg. Sel. Topics Power Electron., vol. 8, no. 1, pp. 805–835, Mar. 2020.

[10] W. Wu, Y. Sun, Z. Lin, T. Tang, F. Blaabjerg, and H. Shu-Hung Chung, "A new LCL-filter with in-series parallel resonant circuit for single phase grid-tied inverter," IEEE Trans. Ind. Electron., vol. 61, no. 9, pp. 4640–4644, Sep. 2014.

[11] W. Li, Y. Gu, H. Luo, W. Cui, X. He, and C. Xia, "Topology review and derivation methodology of single-phase transformerless photovoltaic inverters for leakage current suppression," IEEE Trans. Ind. Electron., vol. 62, no. 7, pp. 4537–4551, Jul. 2015.

[12] L. Concari, D. Barater, C. Concari, A. Toscani, G. Buticchi, and M. Liserre, "H8 architecture for reduced common-mode voltage three phase PV converters with silicon and SiC power switches," in Proc. 43rd Annu. Conf. IEEE Ind. Electron. Soc., Beijing, China, 2017, pp. 4227–4232.